J|A|C|S ARTICLES

Published on Web 07/14/2009

Large Metal Ions in a Relatively Small Fullerene Cage: The Structure of $Gd_3N@C_2(22010)$-C_{78} Departs from the Isolated Pentagon Rule

Christine M. Beavers,[†] Manuel N. Chaur,[‡] Marilyn M. Olmstead,*[,§] Luis Echegoyen,*[,‡] and Alan L. Balch*[,§]

Advanced Light Source, Lawrence Berkeley National Lab, One Cyclotron Road, Berkeley, California 94720, Department of Chemistry, University of California, One Shields Avenue, Davis, California 95616, and Department of Chemistry, Clemson University, Clemson, South Carolina 29634

Received May 7, 2009; E-mail: albalch@ucdavis.edu; mmolmstead@ucdavis.edu; luis@clemson.edu

Abstract: An isomerically pure sample of $Gd_3N@C_{78}$ has been extracted from the carbon soot formed in the electric-arc generation of fullerenes using hollow graphite rods packed with Gd_2O_3 and graphite powder under an atmosphere of helium and dinitrogen. Purification has been achieved by chromatographic methods and the product has been characterized by mass spectrometry, UV/vis absorption spectroscopy, and cyclic voltammetry. Although a number of endohedral fullerenes have been found to utilize the $D_{3h}(5)$-C_{78} cage, comparison of the spectroscopic and electrochemical properties of the previously characterized $Sc_3N@D_{3h}(5)$-C_{78} with those of $Gd_3N@C_{78}$ reveals significant differences that indicate that these two endohedrals do not possess the same cage structure. A single crystal X-ray diffraction study indicates that the fullerene cage does not follow the isolated pentagon rule (IPR) but has two equivalent sites where two pentagons abut. The endohedral has been identified as $Gd_3N@C_2(22010)$-C_{78}. Two of the gadolinium atoms of the planar Gd_3N unit are located within the pentalene folds formed by the adjacent pentagons. The third gadolinium atom resides at the center of a hexagonal face of the fullerene.

Introduction

Fullerenes consist of closed cages of carbon atoms that are arranged into 12 pentagonal rings and a variable number of hexagonal rings, with the number of hexagonal rings increasing as the size of the fullerene increases.[1] The prototypical fullerene, C_{60}, has 20 hexagonal rings along with the required 12 pentagonal rings on its surface. The isolated pentagon rule (IPR) has been successfully used to predict and analyze the structures of numerous empty cage fullerenes and the adducts that they can form.[2] The IPR requires that each of the pentagonal rings in any fullerene is surrounded by hexagonal rings exclusively. This arrangement avoids any direct connections between pentagons and alleviates the strain produced by placing two pentagons adjacent to one another.

Endohedral fullerenes also consist of a closed carbon cage but have an atom, molecule, or other group of atoms trapped inside. Endohedral fullerenes were discovered immediately after the special stability of C_{60} was recognized,[3] and the number of known endohedral fullerenes has been constantly growing.[4,5] Endohedral fullerenes have been shown to encapsulate up to three individual metal atoms and to incorporate various atomic clusters of the types: M_3N,[6] M_2C_2,[7,8] M_3C_2[9] and M_4O_2 where M is an electropositive metal, for example, scandium.[10] Lanthanide ions are readily incorporated into endohedral fullerenes and bring with them potentially useful magnetic, emissive, and nuclear properties. The carbon cage provides firm entrapment of these ions and can serve as the ultimate chelating agent.

In predicting the structure of endohedral fullerenes the IPR seems less of a rule and more of a suggestion,[11] since a growing number of endohedral fullerenes have been found to contain one or more pairs of fused pentagonal rings. Endohedral fullerenes that involve a single pair of fused pentagons include the crystallographically characterized, egg-shaped fullerenes,

[†] Lawrence Berkeley National Lab.
[‡] Clemson University.
[§] University of California.

(1) Fowler, P. W.; Manolopoulos, D. E. *An Atlas of Fullerenes*; Clarendon Press: Oxford, 1995.
(2) Kroto, H. W. *Nature* **1987**, *329*, 529–531.
(3) Heath, J. R.; O'Brien, S. C.; Zhang, Q.; Liu, Y.; Curl, R. F.; Kroto, H. W.; Tittel, F. K.; Smalley, R. E. *J. Am. Chem. Soc.* **1985**, *107*, 7779–7780.
(4) Akasaka, T.; Nagase, S. *Endofullerenes: A New Family of Carbon Clusters*; Kluwer Academic Publishers: Dordrecht, The Netherlands, 2002.
(5) Dunsch, L.; Yang, S. *Small* **2007**, *3*, 1298–1320.
(6) Stevenson, S.; Rice, G.; Glass, T.; Harich, K.; Cromer, F.; Jordan, M. R.; Craft, J.; Hadju, E.; Bible, R.; Olmstead, M. M.; Maitra, K.; Fisher, A. J.; Balch, A. L.; Dorn, H. C. *Nature* **1999**, *401*, 55–57.
(7) Wang, C. R.; Kai, T; Tomiyama, T.; Yoshida, T.; Kobayashi, Y.; Nishibori, E.; Takata, M.; Sakata, M.; Shinohara, H. *Angew. Chem., Int. Ed.* **2001**, *40*, 397–399.
(8) Iiduka, Y.; Wakahara, T.; Nakajima, K.; Nakahodo, T.; Tsuchiya, T.; Maeda, Y.; Akasaka, T.; Yoza, K.; Liu, M. T. H.; Mizorogi, N.; Nagase, S. *Angew. Chem., Int. Ed.* **2007**, *46*, 5562–5564.
(9) Iiduka, Y.; Wakahara, T.; Nakahodo, T.; Tsuchiya, T.; Sakuraba, A.; Maeda, Y.; Akasaka, T.; Yoza, K.; Horn, E.; Kato, T.; Liu, M. T. H.; Mizorogi, N.; Kobayashi, K. *J. Am. Chem. Soc.* **2005**, *127*, 12500–12501.
(10) Stevenson, S.; Mackey, M. A.; Stuart, M. A.; Phillips, J. P.; Easterling, M. L.; Chancellor, C. J.; Olmstead, M. M.; Balch, A. L. *J. Am. Chem. Soc.* **2008**, *130*, 11844–11845.

$Gd_3N@C_s(39663)$-C_{82}[11] and $M_3N@C_s(51365)$-C_{84} (M = Gd, Tb, Tm),[12,13] as well as $La@C_2$-C_{72} (crystallographically characterized as the adduct $La@C_2$-$C_{72}(C_6H_3Cl_2)$).[14] Endohedral fullerenes with two pairs of fused pentagons include $La_2@D_2(10611)$-C_{72}, which has been crystallographically characterized as carbene adducts,[15−17] and $DySc_2N@C_s(17490)C_{76}$.[18] There are several endohedral fullerenes that have three pairs of fused pentagons including: $Sc_2@C_{66}$,[19] and $Sc_3N@C_{2v}(7854)$-C_{70}[20] and crystallographically determined structures for $Sc_3N@D_3(6140)$-C_{68}[21] and $Sc_2C_2@C_{2v}(6073)$-C_{68}.[22] A common feature in all of these endohedrals involves the positioning of metal ions in close proximity to the fused pentagons. Metal ion coordination of isolated pentalene units has been extensively studied by organometallic chemists.[23,24]

Gadolinium as Gd^{3+} with seven unpaired electrons is widely used as a relaxation agent in magnetic resonance imaging (MRI) studies.[25] Endohedral fullerenes containing gadolinium have been shown to function as effective relaxation agents when appropriately functionalized to make them water-soluble.[26,27] The preparation and isolation of new gadolinium containing endohedrals should provide additional paramagnetic molecules for the development of enhanced MRI contrast agents. This article is concerned with the isolation and characterization of a new endohedral, $Gd_3N@C_{78}$, which contains three relatively large gadolinium atoms in a rather small fullerene cage.[28]

As seen in Chart 1, there are five isomers of the C_{78} cage that obey the IPR: one with D_3 symmetry, two with C_{2v} symmetry ($C_{2v}(2)$-C_{78} and $C_{2v}(3)$-C_{78}) and two with D_{3h} symmetry ($D_{3h}(4)$-C_{78}, and $D_{3h}(5)$-C_{78}) and 24105 isomers that do not obey the IPR (but still have a surface comprised of hexagons and 12 pentagons). Three soluble isomers of hollow C_{78} can be extracted from the carbon soot formed in fullerene generation: D_3-C_{78}, $C_{2v}(2)$-C_{78}, and $C_{2v}(3)$-C_{78}.[29−31] Additionally, high temperature trifluoromethylation of arc-generated carbon soot yields an adduct of $D_{3h}(5)$-C_{78}.[32,33] Thus, $D_{3h}(5)$-C_{78} is present in the carbon soot after sublimation and extraction to remove the soluble isomers. There is as yet no evidence for the existence of $D_{3h}(4)$-C_{78} in carbon soot.[34,35]

Chart 1. IPR Isomers of C_{78}

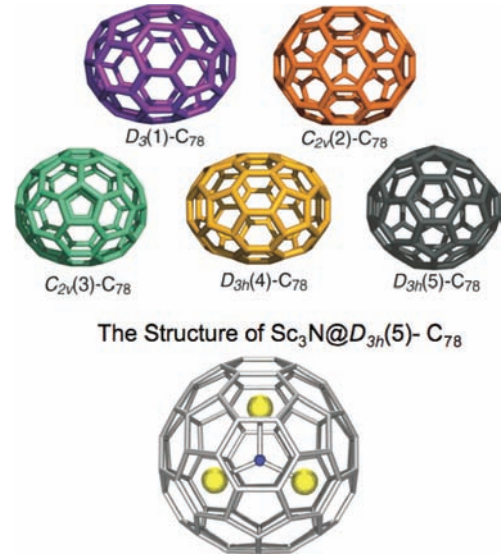

Several endohedral fullerenes have been structurally characterized that employ a C_{78} carbon cage. The majority of these utilize the $D_{3h}(5)$-C_{78} cage. In $Sc_3N@D_{3h}(5)$-C_{78} the planar Sc_3N group lies in the horizontal mirror plane as seen in Chart 1.[36,37] For $La_2@D_{3h}(5)$-C_{78}[38,39] and $Ce_2@D_{3h}(5)$-C_{78},[40] the metal ions

(11) Mercado, B. Q.; Beavers, C. M.; Olmstead, M. M.; Chaur, M. N.; Walker, K.; Holloway, B. C.; Echegoyen, L.; Balch, A. L. *J. Am. Chem. Soc.* **2008**, *130*, 7854–7855.
(12) Beavers, C. M.; Zuo, T.; Duchamp, J. C.; Harich, K.; Dorn, H. C.; Olmstead, M. M.; Balch, A. L. *J. Am. Chem. Soc.* **2006**, *128*, 11352–11353.
(13) Zuo, T.; Walker, K.; Olmstead, M. M.; Melin, F.; Holloway, B. C.; Echegoyen, L.; Dorn, H. C.; Chaur, M. N.; Chancellor, C. J.; Beavers, C. M.; Balch, A. L.; Athans, A. J. *Chem. Commun.* **2008**, 1067–1069.
(14) Wakahara, T.; Nikawa, H.; Kikuchi, T.; Nakahodo, T.; Rahman, G. M. A.; Tsuchiya, T.; Maeda, Y.; Akasaka, T.; Yoza, K.; Horn, E.; Yamamoto, K.; Mizorogi, N.; Slanina, Z.; Nagase, S. *J. Am. Chem. Soc.* **2006**, *128*, 14228–14229.
(15) Kato, H.; Taninaka, A.; Sugai, T.; Shinohara, H. *J. Am. Chem. Soc.* **2003**, *125*, 7782–7783.
(16) Lu, X; Nikawa, H.; Nakahodo, T.; Tsuchiya, T.; Ishitsuka, M. O; Maeda, Y.; Akasaka, T.; Toki, M.; Sawa, H.; Slanina, Z.; Mizorogi, N.; Nagase, S. *J. Am. Chem. Soc.* **2008**, *130*, 9129–9136.
(17) Lu, X.; Nikawa, H.; Tsuchiya, T.; Maeda, Y.; Ishitsuka, M. O.; Akasaka, T.; Toki, M.; Sawa, H.; Slanina, Z.; Mizorogi, N.; Nagase, S. *Angew. Chem., Int. Ed.* **2008**, *47*, 8642–8645.
(18) Yang, S.; Popov, A. A.; Dunsch, L. *J. Phys. Chem. B.* **2007**, *111*, 13659–13663.
(19) Wang, C.-R.; Kai, T.; Tomiyama, T.; Yoshida, T.; Kobayashi, Y.; Nishibori, E.; Takata, M.; Sakata, M.; Shinohara, H. *Nature* **2000**, *408*, 426.
(20) Yang, S. F.; Popov, A. A.; Dunsch, L. *Angew. Chem., Int. Ed.* **2007**, *46*, 1256–1259.
(21) Olmstead, M. M.; Lee, H. M.; Duchamp, J. C.; Stevenson, S.; Marciu, D.; Dorn, H. C.; Balch, A. L. *Angew. Chem., Int. Ed.* **2003**, *42*, 900.
(22) Shi, Z. Q.; Wu, X.; Wang, C. R.; Lu, X.; Shinohara, H. *Angew. Chem., Int. Ed.* **2006**, *45*, 2107.
(23) Summerscales, O. T.; Cloke, F. G. N. *Coord. Chem. Rev.* **2006**, *250*, 1122–1140.
(24) Bendjaballah, S.; Kahlal, S.; Costuas, K.; Bévillon, E.; Saillard, J.-Y. *Chem.—Eur. J.* **2006**, *12*, 2048–2065.
(25) Caravan, P.; Ellison, J. J.; McMurry, T. J.; Lauffer, R. B. *Chem. Rev.* **1999**, *99*, 2293–2352.
(26) Mikawa, M.; Kato, H.; Okumura, M.; Narazaki, M.; Kanazawa, Y.; Miwa, N.; Shinohara, H. *Bioconjugate Chem.* **2001**, *12*, 510–514.
(27) Bolskar, R. D.; Benedetto, A. F.; Husebo, L. O.; Price, R. E.; Jackson, E. F.; Wallace, S.; Wilson, L. J.; Alford, J. M. *J. Am. Chem. Soc.* **2003**, *125*, 5471–5478.
(28) Chaur, M. N.; Melin, F.; Elliott, B.; Athans, A. J.; Walker, K.; Holloway, B. C.; Echegoyen, L. *J. Am. Chem. Soc.* **2007**, *129*, 14826–14829.
(29) Diederich, F.; Whetten, R. L.; Thilgen, C.; Ettl, R.; Chao, I.; Alvarez, M. M. *Science* **1991**, *254*, 1768–1770.
(30) Kikuchi, K.; Nakahara, N.; Wakabayashi, T.; Suzuki, S.; Shiromaru, H.; Miyake, Y.; Saito, K.; Ikemoto, I.; Kainosho, M.; Achiba, Y. *Nature* **1992**, *357*, 142–145.
(31) Taylor, R.; Langley, G. J.; Dennis, T. J. S.; Kroto, H. W.; Walton, D. R. M. *J. Chem. Soc., Chem. Commun.* **1992**, 1043–1044.
(32) Shustova, N. B.; Kuvychko, I. K.; Bolskar, R. D.; Seppelt, K.; Strauss, S. H.; Popov, A. A.; Boltalina, O. V. *J. Am. Chem. Soc.* **2006**, *128*, 15793–15798.
(33) Shustova, N. B.; Newell, B. S.; Miller, S. M.; Anderson, O. P.; Bolskar, R. D.; Seppelt, K.; Popov, A. A.; Boltalina, O. V.; Strauss, S. H. *Angew. Chem., Int. Ed.* **2007**, *46*, 4111–4114.
(34) Kareev, I. E.; Popov, A. A.; Kuvychko, I. V.; Shustova, N.; Lebedkin, S. F.; Bubnov, V. P.; Anderson, O. P.; Seppelt, K.; Strauss, S. H.; Boltalina, O. V. *J. Am. Chem. Soc.* **2008**, *130*, 13471–13489.
(35) (a) Simeonov, K. S.; Amsharov, K. Yu.; Krokos, E.; Jansen, M. *Angew. Chem., Int. Ed.* **2008**, *47*, 6283–6285. (b) Simeonov, K. S.; Amsharov, K.; Yu.; Jansen, M. *Chem.—Eur. J.* **2008**, *14*, 9585–9590. As pointed out in ref 34, the $D_{3h}(5)$-C_{78} carbon cage is present in $C_{78}Cl_{18}$.
(36) Olmstead, M. M.; de Bettencourt-Dias, A.; Duchamp, J. C.; Stevenson, S.; Marcui, D.; Dorn, H. C.; Balch, A. L. *Angew. Chem., Int. Ed.* **2001**, *40*, 1223–1225.
(37) Campanera, J. M.; Bo, C.; Olmstead, M. M.; Balch, A. L.; Poblet, J. M. *J. Phys. Chem. A* **2002**, *106*, 12356–12364.
(38) Cao, B.; Wakahara, T.; Tsuchiya, T.; Kondo, M.; Maeda, Y.; Rahman, G. M. A; Akasaka, T.; Kobayashi, K.; Nagase, S.; Yamamoto, K. *J. Am. Chem. Soc.* **2004**, *126*, 9164–9165.
(39) Cao, B.; Nikawa, H.; Nakahodo, T.; Tsuchiya, T.; Maeda, Y.; Akasaka, T.; Sawa, H.; Slanina, Z.; Mizorogi, N.; Nagase, S. *J. Am. Chem. Soc.* **2008**, *130*, 983–989.

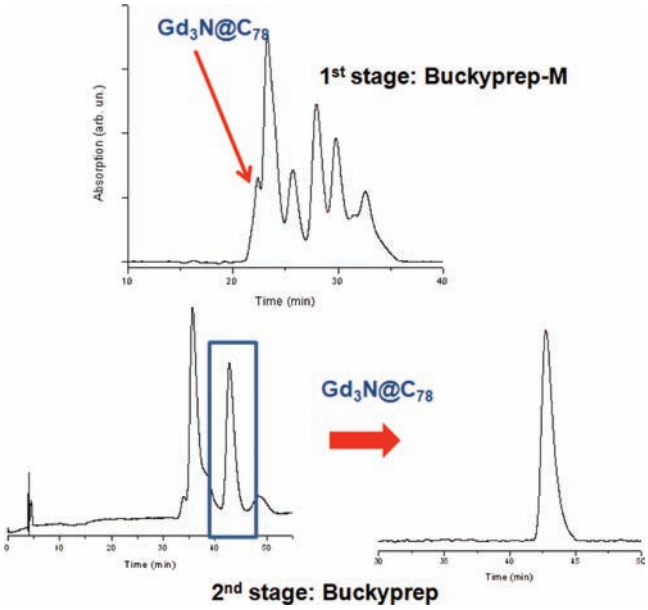

Figure 1. HPLC separation of $Gd_3N@C_2(22010)$-C_{78}. (Upper) Chromatogram from the initial HPLC of extract on a Buckyprep-M column (mobile phase, toluene; flow rate, 4.00 mL/min). (Lower) Chromatogram from the second and third stages on a Buckyprep column (mobile phase, toluene; flow rate, 4.00 mL/min).

lie on the C_3 axis near the polar caps of the carbon cage. This arrangement maximizes the separation between the two metal atoms. Finally reanalysis of the ^{13}C NMR spectrum of Ti_2C_{82} and computational studies indicate that this compound has the metal-carbide structure $Ti_2C_2@D_{3h}(5)$-C_{78}.[41−43] In contrast, computational and infrared studies of the major isomer of $Dy_3N@C_{78}$ and of $Tm_3N@C_{78}$ have suggested that these molecules use the non-IPR fullerene cage isomer $C_2(22010)$-C_{78} as a consequence of the large sizes of Dy^{3+} and Tm^{3+}.[44,45] In this report, we provide the first structural examination of this C_{78} isomer through a single crystal X-ray diffraction study of $Gd_3N@C_2(22010)$-C_{78}.

Results

Isolation of $Gd_3N@C_2(22010)$-C_{78}. Endohedral fullerenes containing Gd_3N units were synthesized in a modified Krätschmer-Huffman arc-discharge reactor as described before.[28] The crude mixture of $Gd_3N@C_{2n}$ metallofullerenes was analyzed by High Performance Liquid Chromatography (HPLC) in a Buckyprep-M column with a toluene flow rate of 4.00 mL/min as shown in Figure 1. The first fraction containing $Gd_3N@C_2(22010)$-C_{78} was collected and then subjected to a second chromatographic purification on a Buckyprep column using toluene as an eluent with a flow rate of 4.00 mL/min. At this point, three different fractions were collected. The middle fraction contained $Gd_3N@C_2(22010)$-C_{78}, and this fraction was analyzed by additional chromatography. No other peaks were detected in this purified sample when it was subjected to chromatography with other columns or a linear combination of columns. The purified sample of $Gd_3N@C_2(22010)$-C_{78} was also analyzed by MALDI-TOF mass spectrometry as shown in Figure 2. As seen in the inserts, the calculated and experimental isotopic distributions matched very well.

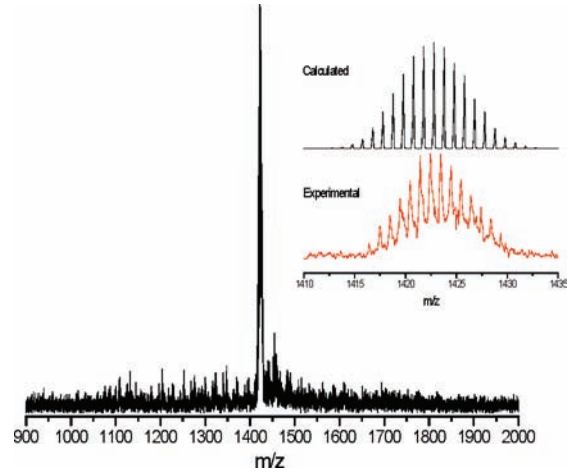

Figure 2. MALDI-TOF mass spectrum of the purified sample of $Gd_3N@C_2(22010)$-C_{78}. (Inset) Expansions of the calculated and experimental spectra for $Gd_3N@C_2(22010)$-C_{78}.

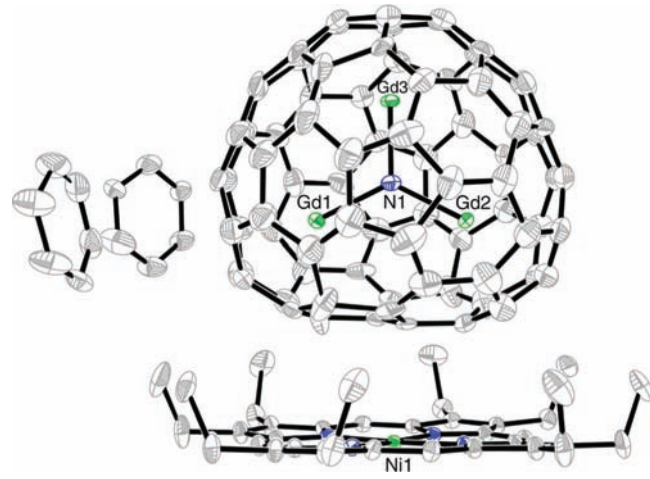

Figure 3. View of the asymmetric unit in crystalline $Gd_3N@C_2(22010)$-C_{78}·Ni^{II}(OEP)·1.5 C_6H_6 that shows the inter-relationship of the fullerene and the nickel porphyrin.

Structure of $Gd_3N@C_2(22010)$-C_{78} as Determined by Single Crystal X-Ray Diffraction. Black crystals of $Gd_3N@C_2(22010)$-C_{78}·Ni(OEP)·1.5C_6H_6 were obtained by the slow diffusion of a solution of 0.4 mg of $Gd_3N@C_2(22010)$-C_{78} dissolved in a minimum of benzene over a benzene solution of Ni^{II}(OEP) in a NMR tube constricted in the middle and kept at 4 °C. Crystals grew during a two week period.

Figure 3 shows the structure of the endohedral fullerene and its relationship to the nickel porphyrin. For C_{78} there are only five isomers that obey the isolated pentagon rule (IPR). However, the fullerene cage in $Gd_3N@C_2(22010)$-C_{78} does not obey the IPR. Rather it has a structure with C_2 symmetry and two locations where two pentagons abut. Figure 4 shows two orthogonal views of the endohedral itself with the abutting pentagons highlighted in turquoise. The cage is disordered. There are four overlapping orientations of the cage with refined

(40) Yamada, M.; Wakahara, T.; Tsuchiya, T.; Maeda, Y.; Kako, M.; Akasaka, T.; Yoza, K.; Horn, E.; Mizorogi, N.; Nagase, S. *Chem. Commun.* **2008**, 558–560.
(41) Cao, B.; Hasegawa, M.; Okada, K.; Tomiyama, T.; Okazaki, T.; Suenaga, K.; Shinohara, H. *J. Am. Chem. Soc.* **2001**, *123*, 9679–9680.
(42) Yumura, T.; Sato, Y.; Suenaga, K.; Iijima, S. *J. Phys. Chem. B* **2005**, *109*, 20251–20255.
(43) Otani, M.; Susumu Okada, S.; Oshiyama, A. *Chem. Phys. Lett.* **2007**, *438*, 274–278.
(44) Popov, A. A.; Krause, M.; Yang, S.; J; Wong, J.; Dunsch, L. *J. Phys. Chem. B* **2007**, *111*, 3363–3369.
(45) Popov, A. A.; Dunsch, L. *J. Am. Chem. Soc.* **2007**, *129*, 11835–11849.

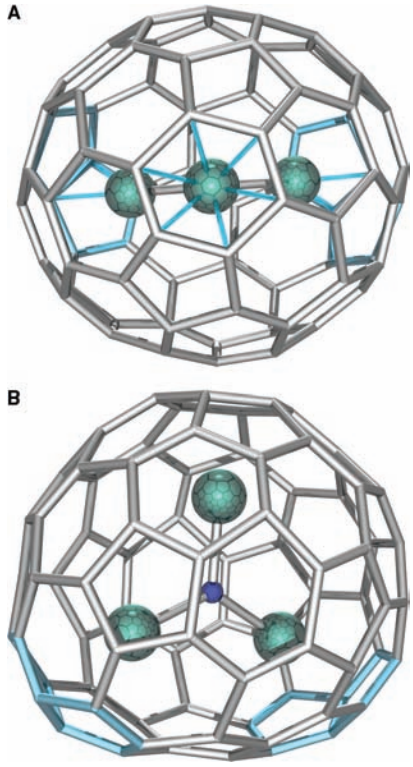

Figure 4. Two orthogonal views of $Gd_3N@C_2(22010)$-C_{78} with abutting pentagons highlighted in turquoise, the nitrogen atom in blue and the gadolinium atoms in green. (A) View down the noncrystallographic 2-fold axis of the carbon cage. (B) Side view with the 2-fold axis in the vertical direction. Only the major gadolinium sites and the major cage orientation are shown.

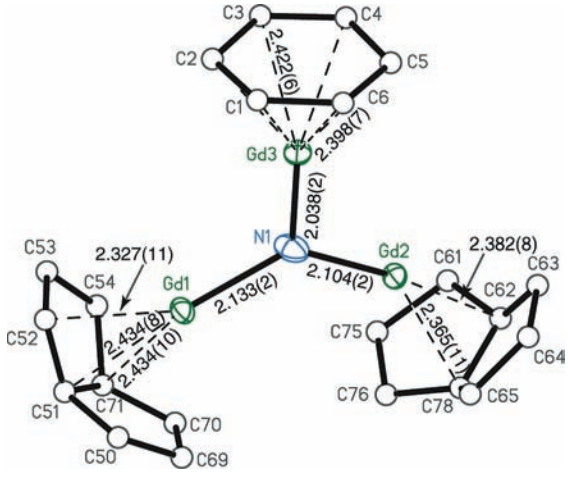

Figure 5. Drawing showing the position of the major Gd_3N unit relative to the nearest carbon atoms of the fullerene cage in $Gd_3N@C_2(22010)$-C_{78}. Distances are given in Å.

occupancies of 0.402(2), 0.232(3), 0.181(3) and 0.184(3). The gadolinium ions are also subject to disorder. The major sites with occupancies of 0.36 for Gd1, 0.23 for Gd2 and 0.25 for Gd3 are shown in Figures 3 and 4 along with the major cage orientation. There are an additional twenty two sites that are fractionally occupied by gadolinium ions.

Figure 5 shows the relationship between the principal Gd_3N site and the adjacent carbon atoms. The Gd−N distances are 2.037(2), 2.103(2) and 2.133(2) Å, which are similar to the Gd−N distances (2.038(8), 2.085(4), and 2.117(5) Å) observed

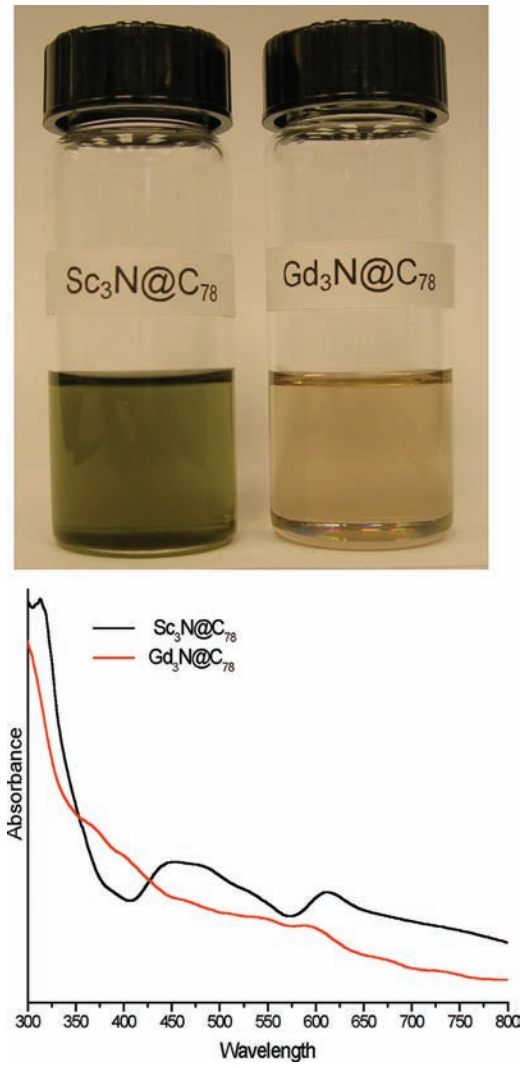

Figure 6. (Upper) Picture of vials containing toluene solutions of $Sc_3N@D_{3h}(5)$-C_{78} and $Gd_3N@C_2(22010)$-C_{78}. (Lower) UV/vis spectra of toluene solutions of $Sc_3N@D_{3h}(5)$-C_{78} and $Gd_3N@C_2(22010)$-C_{78}.

for $Gd_3N@I_h$-C_{80}.[46] In comparison the Sc−N distances in $Sc_3N@D_{3h}(5)$-C_{78} are shorter: 1.981(6), 1.967(15), and 2.127(4) Å. The Gd_3N unit is planar. The sum of the three Gd−N−Gd angles (Gd1−N1−Gd2, 127.37(11); Gd2−N1−Gd3, 116.59(11); Gd1−N1−Gd3 116.03(11) °) is 359.99° and the nitrogen atom is only 0.01 Å out of the Gd_3 plane. As is frequently found for endohedral fullerenes that do not obey the IPR, two of the gadolinium ions are positioned near the pentalene units where the pentagons abut. The other gadolinium ion sits below the center of a hexagon on the fullerene surface, a metal ion position that is frequently seen for other endohedral fullerenes.

The ability of the $C_2(22010)$-C_{78} cage to accommodate a planar Gd_3N unit must provide a significant driving force for the formation of this particular cage isomer. If a Gd_3N unit were placed inside a $D_{3h}(5)$-C_{78} cage, the nitrogen atom would need to be *ca* 0.55 Å out of the Gd_3 plane in order to accommodate the average Gd−N distance of 2.091 Å found in $Gd_3N@C_2(22010)$-C_{78}.

Spectral and Electrochemical Comparisons of $Gd_3N@C_2(22010)$-C_{78} and $Sc_3N@D_{3h}(5)$-C_{78}. Figure 6 presents photographs of

(46) Stevenson, S.; Phillips, J. P.; Reid, J. E.; Olmstead, M. M.; Rath, S. P.; Balch, A. L. *Chem. Comm.* **2004**, 2814–2815.

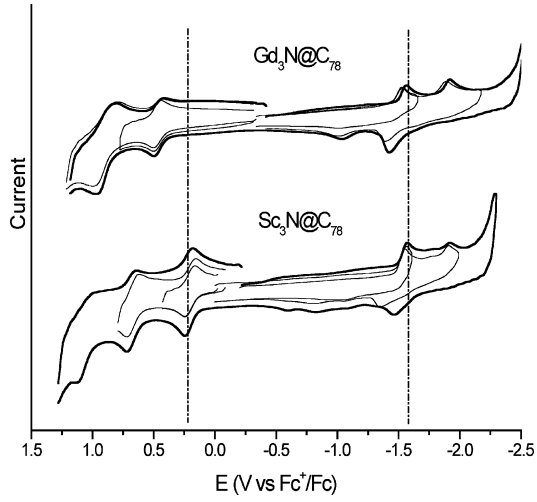

Figure 7. Cyclic voltammograms of $Gd_3N@C_2(22010)$-C_{78} and $Sc_3N@D_{3h}(5)$-C_{78} in 0.05 M (n-Bu_4N)(PF_6) in o-dichlorobenzene with a scan rate of 0.1 V s^{-1}.

Table 1. Peak Potentials vs. Fc^+/Fc for $M_3N@C_{78}$ (M = Gd, Dy and Sc)

MN EMF	$E_{1/2}$ ox1 [V]	$E_{1/2}$ ox2 [V]	E_p ox2 [V]	E_p red1 [V]	E_p red2 [V]	ΔE [V]
$Gd_3N@C_2(22010)$-C_{78}	0.47		1.00	−1.53	−1.89	2.00
$Dy_3N@C_2(22010)$-C_{78}[a]	0.47			−1.54	−1.93	2.01
$Sc_3N@D_{3h}(5)$-C_{78}	0.21	0.68		−1.56	−1.91	1.77

[a] Data from ref 49.

toluene solutions of $Gd_3N@C_2(22010)$-C_{78} and $Sc_3N@D_{3h}(5)$-C_{78} and their UV/vis absorption spectra. It has been known that electronic absorptions of endohedral fullerenes are mostly due to $\pi-\pi^*$ transitions of the fullerene cage.[47] The decidedly distinct absorption characteristics of $Gd_3N@C_2(22010)$-C_{78} and $Sc_3N@D_{3h}(5)$-C_{78} seen in Figure 6 are consisent with the presence of different carbon cage symmetries for each of these endohedral metallofullerenes. The spectrum of $Gd_3N@C_2(22010)$-C_{78} is also similar to those of the major isomer of $Dy_3N@C_{78}$ and $Tm_3N@C_{78}$, whose spectra were reported previously.[44]

Cyclic voltammograms for o-dichlorobenzene solutions of $Gd_3N@C_2(22010)$-C_{78} and $Sc_3N@D_{3h}(5)$-C_{78} with 0.05 M (n-Bu_4N)(PF_6) as supporting electrolyte are shown in Figure 7, while Table 1 contains relevant redox potential data. $Gd_3N@C_2(22010)$-C_{78} exhibits a reversible oxidation wave that is followed by an irreversible second oxidation wave and two irreversible reduction waves. In comparison $Sc_3N@D_{3h}(5)$-C_{78} shows two reversible oxidations and irreversible reduction steps. For both compounds, scanning the cyclic voltammograms at higher rates did not improve the reversibility of the reductive processes. There are major differences in the anodic part of the CVs as seen in Figure 7. The first and second oxidation potentials for $Gd_3N@C_2(22010)$-C_{78} and $Sc_3N@D_{3h}(5)$-C_{78} differ by 260 mV and 320 mV respectively. Echegoyen and co-workers reported that the symmetry of the carbon cage has a remarkable influence on the redox potentials of M_3N-containing endohedral fullerenes.[48] For instance, the D_{5h} and I_h isomers of $Sc_3N@C_{80}$ exhibit a 270 mV difference in the first oxidation potential, and for the second oxidation the difference is even larger (440 mV), with the D_{5h} isomer being easier to oxidize. Thus, the difference in redox potentials observed for $Gd_3N@C_2(22010)$-C_{78} and $Sc_3N@D_{3h}(5)$-C_{78} can be attributed to the difference in cage geometry. Furthermore, the electrochemistry of $Dy_3N@C_{78}$ (whose structure has been suggested to utilize the non-IPR C_2: 22010 cage on the basis of computations and its infrared spectrum)[49] and $Gd_3N@C_2(22010)$-C_{78} are remarkably similar. This observation strongly suggests that these two endohedral fullerenes share the same cage symmetry (see Table 1).

Discussion

$Gd_3N@C_2(22010)$-C_{78} is the smallest of the six Gd_3N-containing endohedrals that have been extracted from the carbon soot formed in the electric-arc generation of fullerenes using hollow graphite rods packed with Gd_2O_3 and graphite powder.[28] The other endohedrals formed include: $Gd_3N@I_h$-C_{80}, $Gd_3N@C_s(39663)$-C_{82}, $Gd_3N@C_s(51365)$-C_{84}, $Gd_3N@C_{86}$, and $Gd_3N@C_{88}$. Of these six, published crystallographic studies have shown that $Gd_3N@I_h$-C_{80} follows the IPR and contains a pyramidalized Gd_3N unit with the nitrogen atom 0.522(8) Å away from the Gd_3 plane.[50] In contrast, $Gd_3N@C_2(22010)$-C_{78}, $Gd_3N@C_s(39663)$-C_{82},[11] and $Gd_3N@C_s(51365)$-C_{84}[13] do not obey the IPR but contain planar Gd_3N units.

Metal ions play a role in determining the distribution of sizes of the fullerene cages that are formed in the electric arc process of fullerene generation. For M_3N-containing endohedrals, larger metal ions favor the formation of larger cages. Thus, with scandium, a family of four Sc_3N-containing endohedrals are produced: $Sc_3N@C_{68}$, $Sc_3N@C_{70}$, and two isomers of $Sc_3N@C_{80}$ with $Sc_3N@I_h$-C_{80} as the predominant product.[6] With gadolinium, six endohedrals are formed: $Gd_3N@C_{78}$, $Gd_3N@C_{80}$, $Gd_3N@C_{82}$, $Gd_3N@C_{84}$, $Gd_3N@C_{86}$, and $Gd_3N@C_{88}$.[28]

Generally, for a particular cage size, the metal ion involved has not been found to alter the cage geometry. Thus, the major isomers found for $Gd_3N@C_{84}$, $Tb_3N@C_{84}$ and $Tm_3N@C_{84}$ all utilize the $C_s(51365)$-C_{84} cage despite the fact that there are 24 IPR and 51568 non-IPR isomers available for a C_{84} cage. Likewise, the predominant isomer for endohedrals of the $M_3N@C_{80}$ class utilizes the I_h-C_{80} cage to encapsulate a variety of different M_3N units including: homometallic groups; Sc_3N,[6,50] Lu_3N,[50] Gd_3N,[46] Tb_3N,[51] Tm_3N,[52] Dy_3N,[53] as well as heterometallic units; $ErSc_2N@$,[54] $CeSc_2N$,[55] $GdSc_2N$,[56] Gd_2ScN,[55] $TbSc_2N$.[56] The less abundant isomer of the $M_3N@C_{80}$ class utilizes the D_{5h}-C_{80} cage to encapsulate Sc_3N,[57] Tb_3N,[52] and Tm_3N units.[52] The major isomers of $Ca@C_{3v}$-C_{94} and $Tm@C_{3v}$-

(47) Shinohara, H. *Rep. Prog. Phys.* **2000**, *63*, 843–892.
(48) Elliott, B.; Yu, L.; Echegoyen, L. *J. Am. Chem. Soc.* **2005**, *127*, 10885–10888.
(49) Yang, S.; Zalibera, M.; Rapta, P.; Dunsch, L. *Chem.—Eur. J.* **2006**, *12*, 7848–7863.
(50) Stevenson, S.; Lee, H. M.; Olmstead, M. M.; Kozikowski, C.; Stevenson, P.; Balch, A. L. *Chem.—Eur. J.* **2002**, *8*, 4528–4535.
(51) Zuo, T.; Beavers, C. M.; Duchamp, J. C.; Campbell, A.; Dorn, H. C.; Olmstead, M. M.; Balch, A. L. *J. Am. Chem. Soc.* **2007**, *129*, 2035–2043.
(52) Zuo, T.; Olmstead, M. M.; Beavers, C. M.; Balch, A. L.; Wang, G.; Yee, G. T.; Shu, C.; Xu, L.; Elliot, B.; Echegoyen, L.; Duchamp, J. C.; Dorn, H. C. *Inorg. Chem.* **2008**, *47*, 5234–5244.
(53) Yang, S.; Troyanov, S. I.; Popov, A. A.; Krause, M.; Dunsch, L. *J. Am. Chem. Soc.* **2006**, *128*, 16733–16739.
(54) Olmstead, M. M.; de Bettencourt-Dias, A.; Duchamp, J. C.; Stevenson, S.; Dorn, H. C.; Balch, A. L. *J. Am. Chem. Soc.* **2000**, *122*, 12220–12226.
(55) Wang, X.; Zuo, T.; Olmstead, M. M.; Duchamp, J. C.; Glass, T. E.; Cromer, T. E.; Balch, A. L.; H. C; Dorn, H. C. *J. Am. Chem. Soc.* **2006**, *128*, 8884–8889.
(56) Stevenson, S.; Chancellor, C. J.; Lee, H. M.; Olmstead, M. M.; Balch, A. L. *Inorg. Chem.* **2008**, *47*, 1420–1427.
(57) Cai, T.; Xu, L.; Anderson, M. R.; Ge, Z.; Zuo, T.; Wang, X.; Olmstead, M. M.; Balch, A. L.; Gibson, H. W.; Dorn, H. C. *J. Am. Chem. Soc.*, **2006**, *128*, 8581–8589.

C_{94} have been shown to use the C_{3v}-C_{94} cage.[58] Finally, despite the wide variation in internal composition, the endohedrals—$La_2@C_{78}$, $Ce_2@C_{78}$, $Sc_3N@C_{78}$, and $Ti_2C_2@C_{78}$—all utilize the same $D_{3h}(5)$-C_{78} cage.

The situation with $Gd_3N@C_2(22010)$-C_{78} is clearly different. Despite the similarity in internal composition, unique cages are found for $Gd_3N@C_2(22010)$-C_{78} and $Sc_3N@D_{3h}(5)$-C_{78}. The ability of the $C_2(22010)$-C_{78} cage to accommodate a planar Gd_3N unit appears to be a major factor in the stabilization of this particular fullerene cage.

Experimental Section

Crystallographic Data Collection and Refinement for $Gd_3N@C_2(22010)$-C_{78}·Ni(OEP)·1.5C_6H_6. A black block of dimensions 0.110 × 0.090 × 0.085 mm was mounted in the 90(2) K nitrogen cold stream provided by an Oxford Cryostream low temperature apparatus on the goniometer head of a Bruker D8 diffractometer equipped with an ApexII CCD detector, on beamline 11.3.1 at the Advanced Light Source in Berkeley, CA. Diffraction data were collected using synchrotron radiation monochromated with silicon(111) to a wavelength of 0.77490 Å. An approximate full sphere of data to $2\theta = 103°$ was collected using 0.3° ω scans. A multiscan absorption correction was applied using the program SADABS-2008/1.[59] A total of 567829 reflections were collected, of which 63384 were unique [R(int) = 0.0658] and 47323 were observed [$I > 2\sigma$ (I)]. The structure was solved by direct methods (SHELXS) and refined by full-matrix least-squares on F^2 (SHELXL97)[59] using 3528 parameters.

The fullerene cage is chiral; two orientations of each enantiomer are present within the structure. The fullerene cage of one enantiomer was first identified and determined to have C_2 symmetry. Symmetry related geometric restraints were applied on related 1−2 and 1−3 distances, and the occupancy was decreased to allow the identification of a second orientation, which had the opposite enantiomeric geometry. This process was repeated and allowed the identification of four cage orientations. All four of the cages were kept isotropic with thermal parameter similarity restraints, while the cage occupancies were refined and summed to one. Once the occupancies had converged, the cage carbon atoms of the major site were refined anisotropically, while the carbon atoms of the other three cages remained isotropic. The cage occupancies refined to 0.402(2), 0.232(3), 0.181(3) and 0.184(3). Due to the high level of overlap, refining the major cage anisotropically without the similarity restraints was not possible. Evidence for more, but decidedly minor, orientations of the cages is visible in the difference map, but these were not modeled.

The cage contents, Gd_3N, are also highly disordered, although the nitrogen atom position is unique. The trigonal planar unit Gd_3N appears to rotate about the 2-fold axis of the fullerene, giving a spherical region of density that corresponds to one Gd and a toroidal region that corresponds to the other two. To accurately refine the Gd sites occupancies, the occupancies of the sites within the toroidal region were summed to 2, and the occupancies of the spherical region were summed to 1. Once the occupancies had converged, they were fixed at those values. Twenty-five Gd sites were refined. Only Gd1, Gd2 and Gd3 were identifiable as a viable Gd_3N set; this set corresponds primarily to the major cage. The occupancies of Gd1, Gd2 and Gd3 were 0.36, 0.23, and 0.25 respectively. The difference in their occupancies is due to the other possible combinations of Gd sites that correspond to other cage orientations, some of which have not been modeled. Only Gd sites with occupancies greater than 5% were refined anisotropically.

The hydrogen atoms were generated geometrically and refined as riding atoms with C−H distances = 0.95−0.99 Å and U_{iso}(H) = 1.2 times U_{eq}(C) for CH and CH_2 groups and U_{iso}(H) = 1.5 times U_{eq}(C) for CH_3 groups. The maximum and minimum peaks in the final difference Fourier map were 4.874 and −2.795 eÅ^{-3}.

Crystal Data. $C_{123}H_{53}N_5NiGd$, M_w = 2131.16 amu, monoclinic, *C2/c*, a = 24.9897(6) Å, b = 15.0876(4) Å, c = 39.2517(10) Å, β = 94.2080(10)°, V = 14759.4(6) Å^3, T = 90(2) K, Z = 8, $R1$ [$I > 2\sigma$ (I)] = 0.0960, wR_2 (all data) = 0.3026, GOF (on F^2) = 1.017.

Acknowledgment. We thank the National Science Foundation [CHE-0716843 to A.L.B. and M.M.O. and DMR-0809129 to L.E.)] for support. This material is based on work supported by the National Science Foundation while L.E. was working there. The receipt of crude mixtures of $Sc_3N@C_{2n}$ and $Gd_3N@C_{2n}$ from LUNA Innovation was appreciated. The Advanced Light Source is supported by the Director, Office of Science, Office of Basic Energy Sciences, of the U.S. Department of Energy under Contract No. DE-AC02-05CH11231.

Supporting Information Available: X-ray crystallographic files in CIF format for $Gd_3N@C_2(22010)$-C_{78}·Ni(OEP)·1.5C_6H_6. This material is available free of charge via the Internet at http://pubs.acs.org.

JA903741R

(58) Che, Y.; Yang, H.; Wang, Z.; Jin, H.; Liu, Z.; Lu, C.; Zuo, T.; Dorn, H. C.; Beavers, C. M.; Olmstead, M. M.; Balch, A. L. *Inorg. Chem.* **2009**, *48*, 6004–6010.

(59) Sheldrick, G. M. *Acta Crystallographica Sect. A.* **2008**, *64*, 112.